Korean J. Chem. Eng., 38(12), 2510-2518 (2021)
DOI: 10.1007/s11814-021-0920-3

pISSN: 0256-1115
eISSN: 1975-7220

Purification of durene from the mixture of durene and isodurene by stripping crystallization

Lie-Ding Shiau[*,**,†]

*Department of Chemical and Materials Engineering, Chang Gung University, Taoyuan 333, Taiwan
**Department of Urology, Linkou Chang Gung Memorial Hospital, Taoyuan 333, Taiwan
(*Received 18 April 2021 • Revised 1 August 2021 • Accepted 8 August 2021*)

Abstract−Stripping crystallization (SC) is introduced in this work to purify durene from the mixture consisting of isodurene and durene. SC is a new technology which combines melt crystallization and vaporization via a series of three-phase transformations at low pressures during the cooling process. The three-phase transformation conditions for a liquid mixture determined by the thermodynamic calculations were adopted to direct the batch SC experiments. A model based on the mass and energy balances was proposed to determine the variation of the amount of remaining liquid, crystallized durene product and produced vapor during SC. The experimental yield and purity of the final durene product obtained from the experiments were compared with those predicted by the model.

Keywords: Crystallization, Vaporization, Purification, Thermodynamics Process

INTRODUCTION

Durene, or 1,2,4,5-Tetramethylbenzene, is an important chemical intermediate for producing pyromellitic dianhydride (PMDA), which can be used in the preparation of heat-resistant polyimide for diverse applications [1]. Durene has attracted more and more attention due to the increasing demand for PMDA. As isodurene, or 1,2,3,5-tetramethylbenzene, is often produced from the synthesis of durene, it is an important to separate these two isomers. Due to the close boiling points of durene (196.8 °C) and isodurene (195.6 °C), it is very difficult to separate them by conventional distillation. Static melt crystallization has been proposed to separate these two compounds [2].

A new separation technology, stripping crystallization (SC), has been introduced to separate some mixtures with close boiling temperature, including the mixed xylenes [4-7], the benzene/cyclohexane mixtures [8], and the enantiomer mixtures [9,10]. As opposed to the solid-liquid transformation occurring at normal pressure during the cooling process of melt crystallization [11-22], a series of three-phase transformations occur at low pressure during the SC cooling process [4-10]. In principle, SC combines melt crystallization and vaporization operated for a liquid mixture via a series of three-phase transformations, by which the unwanted components are vaporized from the liquid mixture, while the desired component is crystallized as the solid product. At the end of SC, the crystalline product of the desired component is obtained after the liquid mixture disappears and the vapor is removed. Thus, no solid/liquid separation and no crystal washing is required since no mother liquor is present with final crystals at the end. In the present study SC was applied to purify durene from the durene/isodurene mixture. A model was proposed based on the mass and energy balances to describe the variation of the amounts of remaining liquid mixture, crystallized durene product and vapor produced during the SC cooling process. The experimental results were compared with the calculated results from the proposed model.

PRINCIPLE OF SC

The basic principle of the SC process can be explained by referring to the phase diagrams. Fig. 1 illustrates the phase diagram of isodurene (A-component) and durene (B-component) at normal

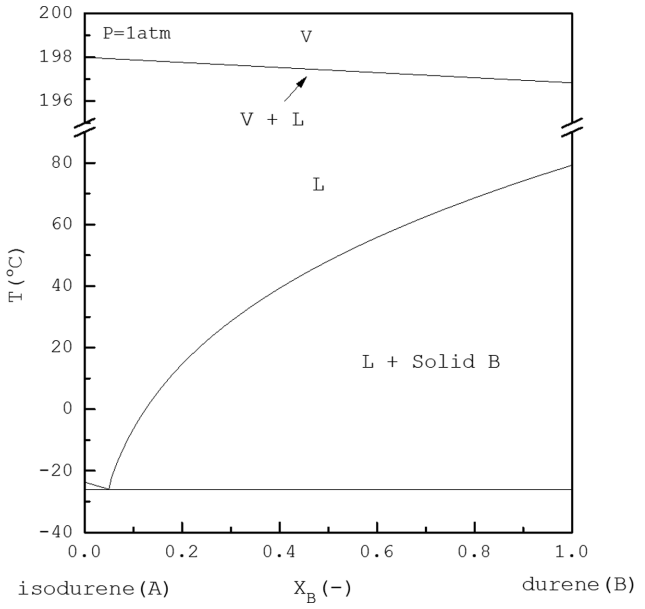

Fig. 1. Phase diagram of isodurene (component-A) and durene (component-B) at P=1 atm.

†To whom correspondence should be addressed.
E-mail: shiau@mail.cgu.edu.tw

Table 1. Some physical properties for isodurene and durene [23]

Property	Isodurene	Durene
IUPAC name	1,2,3,5-Tetramethylbenzene	1,2,4,5-Tetramethylbenzene
Molecular weight	134.22	134.22
T_b (°C)	198	196.8
T_m (°C)	−23.7	79.2
P_{tri} (Pa)	0.105	1,555
ΔH_m (J/mol)	1.29×10^4	2.10×10^4
ΔH_V (J/mol)	5.00×10^4	4.94×10^4

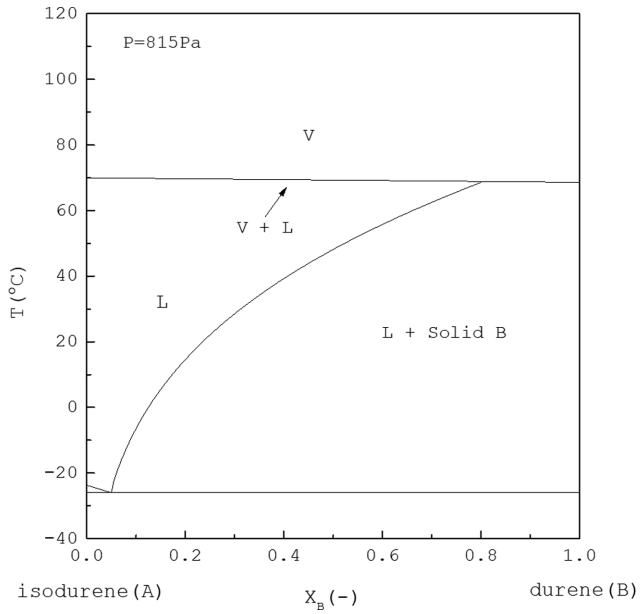

Fig. 2. Phase diagram of isodurene (component-A) and durene (component-B) at P=815 Pa.

pressure. The solid-liquid equilibrium (SLE) is predicted by the van't Hoff equation. Note that the eutectic point lies at X_B=0.05 and T=−26 °C. Some physical properties of isodurene and durene are listed in Table 1 [23].

As the pressure is reduced, the SLE boundaries typically remain nearly unchanged, while the vapor-liquid equilibrium (VLE) boundaries are moved downward. As the pressure is reduced below the triple-point pressure of durene (1,555 Pa), it leads to the existence of a three-phase state having the durene crystalline product, and liquid phase and vapor phase of mixture. Thus, the durene crystalline product is obtained via the three-phase transformation. For example, Fig. 2 illustrates the phase diagram of isodurene and durene at P=815 Pa, where the three-phase state occurs at X_B=0.8 and T=70 °C.

SC MODEL

When SC is applied to purify durene from the liquid mixture consisting of isodurene and durene in the range $0.05<X_B<1$, the SC process is simulated in a series of stage operations shown in Fig. 3, which can also be an abstract representation of a batch process in a single vessel. During the SC cooling process, the temperature of each stage is chosen to meet $T_{n-1}-T_n=\Delta T$ (n=1, 2, …, N) and each stage is operated at the three-phase transformation condition having the durene crystalline product, along with the liquid phase and vapor phase of the mixture. The vapor formed in each stage is condensed to the liquid and removed while the solid crystalline product and the liquid formed in each stage enter the next stage.

As the three-phase transformation occurs in each stage, both the SLE and VLE equations need to be satisfied in each stage. The SLE between the durene crystalline product and liquid mixture in stage n is described by the van't Hoff equation as [24,25]

$$\ln[(X_B)_n]=\frac{\Delta H_{m,B}}{R}\left(\frac{1}{T_{m,B}}-\frac{1}{T_n}\right) \quad (1)$$

The ideal liquid solution is assumed for simplicity due to the structure similarity between isodurene and durene. Due to low pressures, the ideal gas law is assumed for the vapor. Thus, the VLE in stage n (n=1, 2, …, N) can be described by Raoult's law as [24,25]

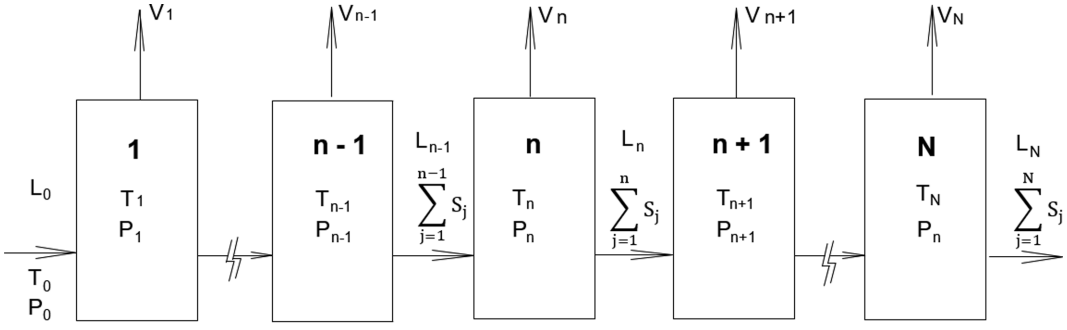

Fig. 3. Schematic diagram of the SC operation where each stage is operated at a three-phase transformation state.

Table 2. Constants of the Antoine equation, $\log_{10}P^{sat}=a-\left(\frac{b}{c+T}\right)$ (P^{sat} in bar and T in K), for isodurene and durene [23]

Constants	Isodurene	Durene
A	3.71768	2.9204
B	1,334.012	908.263
C	−111.909	−160.447

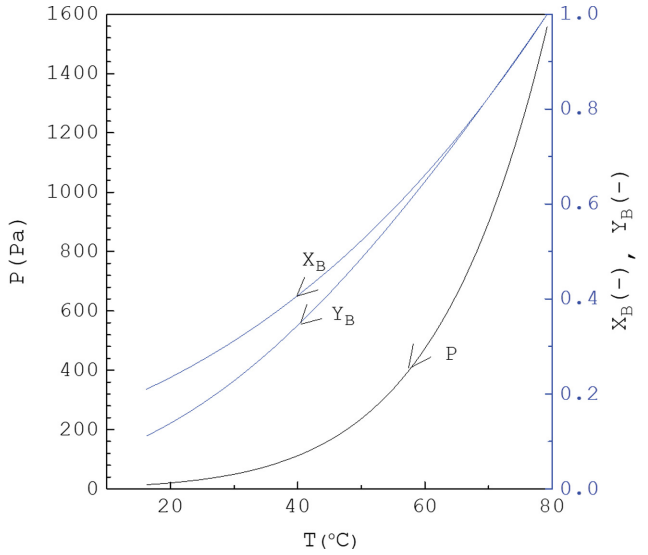

Fig. 4. Calculated results of P(T), X_B(T) and Y_B(T) for the three-phase transformation during the SC cooling process.

$$(Y_A)_n P_n=(X_A)_n(P_A^{sat})_n \quad (2)$$

$$(Y_B)_n P_n=(X_B)_n(P_B^{sat})_n \quad (3)$$

where P_A^{sat} and P_B^{sat} are the temperature-dependent saturated pressure for isodurene and durene, respectively, which are given by the Antoine equation in Table 2. Note that $(X_A)_n+(X_B)_n=1$ and $(Y_A)_n+(Y_B)_n=1$.

Combining Eqs. (2) and (3) yields

$$P_n=(X_A)_n(P_A^{sat})_n+(X_B)_n(P_B^{sat})_n \quad (4)$$

Thus, if T_n is specified, $(X_B)_n$ is determined from Eq. (1) and one has $(X_A)_n=(X_B)_n$; subsequently, as P_n is determined from Eq. (4), $(Y_A)_n$ and $(Y_B)_n$ are determined from Eqs. (2) and (3), respectively. Fig. 4 displays the variations of P, X_B and Y_B during the SC cooling process. Thus, P and X_B decrease as temperature decreases, so as X_B in the liquid mixture decreases, the corresponding temperature and pressure for a series of three-phase transformations decrease.

If the feed is a liquid mixture only, one has L_0 with an initial concentration $(X_B)_0$, leading to $S_0=V_0=0$. The initial three-phase transformation temperature and pressure for the liquid feed, T_0 and P_0, are determined as follows: (a) T_0 is determined for $(X_B)_0$ based on Eq. (1); (b) P_0 is determined for $(X_B)_0$ at T_0 based on Eq. (4). Once T_0 is determined, T_n in each stage can be specified for $T_{n-1}-T_n=\Delta T$ and a chosen ΔT. Consequently, as each stage is operated at the three-phase transformation condition, P_n, $(X_A)_n$, $(X_B)_n$, $(Y_A)_n$ and $(Y_B)_n$ in each sage are determined from Eqs. (1)-(4).

In Fig. 3, S_n represents the amount of the durene crystalline product produced in stage n; L_n represents the amount of the liquid mixture remained in stage n; and V_n represents the amount of vapor formed and removed in stage n. As each stage is operated at the three-phase transformation condition, the operating pressure in each stage needs to be controlled at P(T) depicted in Fig. 4. Subsequently, the produced durene crystalline product and remaining liquid mixture are kept in the stage process, while the vapor formed is removed from the stage process to keep the operating pressure at P(T). The entire material balance in stage n can be described by

$$L_{n-1}=S_n+L_n+V_n \quad (5)$$

As it is assumed that no isodurene is incorporated into the durene crystalline product, the material balance of durene in stage n can be described by

$$L_{n-1}(X_B)_{n-1}=S_n+L_n(X_B)_n+V_n(Y_B)_n \quad (6)$$

It was observed during the experiments that a three-phase transformation occurred in the liquid mixture very quickly in each stage, leading to the formation of the durene crystalline product and the mixture vapor. Therefore, it is assumed in each stage that the heat released in forming the durene crystalline product was quickly removed by vaporizing some portion of the liquid mixture. Thus, the energy balance in stage n can be described by

$$S_n\Delta H_{m,B}=V_n[(Y_A)_n\Delta H_{V,A}+(Y_B)_n\Delta H_{V,B}] \quad (7)$$

where S_n represents the amount of the durene crystalline product crystallized in stage n while V_n represents the amount of the liquid mixture vaporized in stage m. As only durene is crystallized in each stage, $\Delta H_{m,B}$ represents the heat of crystallization for the formation of durene crystals. On the other hand, as the vapor consists of isodurene and durene, $(Y_A)_n\Delta H_{V,A}+(Y_B)_n\Delta H_{V,B}$ represents the heat of vaporization for the vapor formed in stage n.

As in each stage is specified, $(X_B)_n$ and $(Y_B)_n$ are determined previously from Eqs. (1)-(4). If L_{n-1} is known, Eqs. (5)-(7) constitute a set of differential equations that can be simultaneously solved for L_n, S_n, and V_n in stage n (n=1, 2, …, N). To solve for V_n, combining Eqs. (5)-(7) yields

$$V_n=\frac{L_{n-1}[(X_B)_{n-1}-(X_B)_n]}{(Y_B)_n-(X_B)_n+[(Y_A)_n f_A+(Y_B)_n f_B](X_A)_n} \quad (8)$$

where $f_A=\Delta H_{V,A}/\Delta H_{m,B}$ and $f_B=\Delta H_{V,B}/\Delta H_{m,B}$. Once V_n is determined, S_n can be calculated from Eq. (7) and, subsequently, L_n can be calculated from Eq. (5). By definition, one has $S_{tot,n}=\Sigma_{j=1}^{n}S_j$ and $V_{tot,n}=\Sigma_{j=1}^{n}V_j$. Thus, L_N represents the total amount of liquid mixture remaining at the end of SC, while $S_{tot,N}$ and $V_{tot,N}$ represent the total amount of solid crystalline product and the total amount of vapor produced at the end of SC, respectively.

EXPERIMENTAL

The SC experiments were performed using the experimental assembly in Fig. 5, which consists of a 50-mL sample container in a 1.5-L stainless chamber immersed in a constant temperature bath. A pressure gauge was connected to the big chamber and a tem-

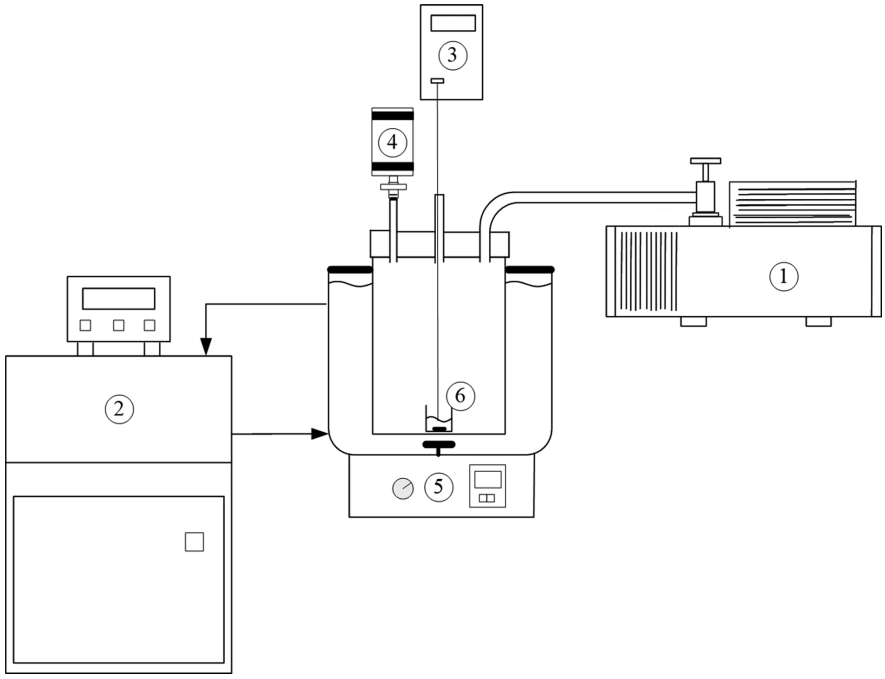

Fig. 5. Schematic diagram of the experimental apparatus for SC with the features: (1) magnetic-driven motor, (2) rotating scraper, (3) sample container, (4) sample, (5) coolant jacket, (6) cooling system, (7) turbomolecular pump, (8) mechanical pump, (9) thermocouple, (10) pressure gauge, (11) transparent cover.

perature probe was positioned in the liquid mixture. The operating temperature and pressure in the chamber during the cooling process were adjusted by controlling the mechanical vacuum pump and constant temperature bath, respectively. Crystallization and vaporization of the liquid mixture during a series of three-phase transformations was observed in the chamber via transparent cover.

Durene (purity >99%) and isodurene (purity >83%) were purchased from Tokyo Chemical Industry. To purify durene from the liquid mixture consisting of isodurene and durene, an initial three-phase transformation generally occurred slightly below the triple-point of durene (T_{tri}=79.2 °C, P_{tri}=1,555 Pa). Once the initial three-phase transformation temperature and pressure for the liquid feed were reached, P(T) in Fig. 3 was adopted during the cooling process to control the operating pressure in the chamber for a series of three-phase transformations.

In the beginning of the experiments, 10 g liquid feed was injected into the sample container stirred by the magnetic-driven motor at 120 rpm. As the temperature decreased at 0.9 °C/min in the chamber, the corresponding operating pressure was reduced by controlling the vacuum pump in keeping with the three-phase transformation conditions. Consequently, a series of three-phase transformations occurred in the liquid mixture, resulting in the formation of the durene crystalline product and mixture vapor. The produced durene crystalline product and remaining liquid were kept in the sample container, while the produced vapor was removed from the chamber to control the pressure in the chamber operated at P(T). Upon completion, the final product ($W_{f,exp}$), including the crystalline product and remaining liquid, in the sample container was weighed. The product purity ($Z_{B,exp}$) was determined by GC using a Perkin-Elmer Clarus 500 series gas chromatograph with a stainless steel capillary column [Bentone 34/DNDP SCOT, 50 ft×0.02 in. (i.d.), Supelco, USA].

RESULTS AND DISCUSSION

SC was applied to purify durene from 10 g liquid feed with $(X_B)_0$=0.80-0.95. Table 3 lists the calculated results for L_0=10 g with $(X_B)_0$=0.80 using ΔT=2 °C for n=1-10, ΔT=4 °C for n=11-15, and ΔT=6 °C for n=16-17, respectively. As the variation of L_n becomes smaller during the later cooling stage, a greater ΔT is chosen during the later cooling stage in the calculations. For n=0, T_0=68.6 °C and P_0=823 Pa corresponds to the initial three-phase transformation condition. As n increases, both T_n and P_n decrease. For n=N (N=17), T_N=16.6 °C and P_N=15 Pa corresponds to the final three-phase transformation condition. As n increases, L_n decreases, while both $S_{tot,n}$ and $V_{tot,n}$ increase. Based on the total material balance, one obtains $L_0=L_n+S_{tot,n}+V_{tot,n}$ in each stage. If SC is operated from 68.6 °C and 823 Pa to 16.6 °C and 15 Pa, the model predicts L_N=1.29 g, $S_{tot,N}$=6.12 g, and $V_{tot,n}$=2.59 g at the end of SC.

Similarly, Table 4 lists the calculated results for L_0=10 g with $(X_B)_0$=0.85, which indicates that, if SC is operated from 71.4 °C and 980 Pa to 19.4 °C and 19 Pa (N=17), the model predicts L_N=0.89 g, $S_{tot,N}$=6.42 g and $V_{tot,N}$=2.72 g at the end of SC. Table 5 lists the calculated results for L_0=10 g with $(X_B)_0$=0.90, which indicates that, if SC is operated from 74.1 °C and 1,154 Pa to 22.1 °C and 25 Pa (N=17), the model predicts L_N=0.48 g, $S_{tot,N}$=6.68 g and $V_{tot,N}$=2.83 g at the end of SC. Table 6 lists the calculated results for L_0=10 g with $(X_B)_0$=0.95, which indicates that, if SC is operated from 76.7 °C and 1,347 Pa to 29.7 °C and 49 Pa (N=17), the model predicts L_N=0.19 g, $S_{tot,N}$=6.88 g and $V_{tot,N}$=2.92 g at the end of SC.

Table 3. Calculated results for L_0=10 g with $(X_B)_0$=0.80 using ΔT=2 °C for n=1-10, ΔT=4 °C for n=11-15, and ΔT=6 °C for n=16-17, respectively

n	T_n (°C)	P_n (Pa)	$(X_B)_n$	$(Y_B)_n$	L_n (g)	S_n (g)	$S_{tot,n}$ (g)	V_n (g)	$V_{tot,n}$ (g)
0	68.6	823	0.800	0.799	10.0	0	0	0	0
1	66.6	726	0.766	0.763	7.92	1.46	1.46	0.62	0.62
2	64.6	639	0.733	0.727	6.51	0.99	2.45	0.42	1.04
3	62.6	561	0.701	0.692	5.51	0.70	3.16	0.30	1.34
4	60.6	492	0.670	0.657	4.76	0.52	3.68	0.22	1.56
5	58.6	430	0.640	0.623	4.19	0.40	4.08	0.17	1.73
6	56.6	376	0.611	0.590	3.73	0.32	4.40	0.13	1.86
7	54.6	328	0.583	0.558	3.37	0.26	4.66	0.11	1.97
8	52.6	285	0.556	0.526	3.07	0.21	4.87	0.09	2.06
9	50.6	247	0.530	0.495	2.82	0.18	5.05	0.07	2.14
10	48.6	214	0.505	0.465	2.61	0.15	5.19	0.06	2.20
11	44.6	159	0.458	0.407	2.27	0.24	5.43	0.10	2.30
12	40.6	117	0.414	0.352	2.01	0.18	5.61	0.08	2.38
13	36.6	86	0.373	0.302	1.82	0.14	5.75	0.06	2.43
14	32.6	62	0.335	0.256	1.66	0.11	5.86	0.05	2.48
15	28.6	44	0.300	0.214	1.54	0.09	5.94	0.04	2.52
16	22.6	26	0.253	0.159	1.40	0.10	6.05	0.04	2.56
17	16.6	15	0.212	0.114	1.29	0.08	6.12	0.03	2.59

Table 4. Calculated results for L_0=10 g with $(X_B)_0$=0.85 using ΔT=2 °C for n=1-10, ΔT=4 °C for n=11-15, and ΔT=6 °C for n=16-17, respectively

n	T_n (°C)	P_n (Pa)	$(X_B)_n$	$(Y_B)_n$	L_n (g)	S_n (g)	$S_{tot,n}$ (g)	V_n (g)	$V_{tot,n}$ (g)
0	71.4	980	0.850	0.851	10.0	0	0	0	0
1	69.4	867	0.814	0.814	7.27	1.92	1.92	0.81	0.81
2	67.4	765	0.780	0.778	5.64	1.14	3.06	0.49	1.30
3	65.4	674	0.746	0.742	4.57	0.75	3.81	0.32	1.62
4	63.4	592	0.714	0.706	3.82	0.52	4.34	0.22	1.84
5	61.4	520	0.683	0.672	3.28	0.38	4.72	0.16	2.00
6	59.4	455	0.652	0.637	2.86	0.29	5.01	0.12	2.12
7	57.4	398	0.623	0.604	2.54	0.23	5.24	0.10	2.22
8	55.4	347	0.595	0.571	2.28	0.18	5.42	0.08	2.30
9	53.4	302	0.567	0.539	2.07	0.15	5.57	0.06	2.36
10	51.4	262	0.541	0.508	1.90	0.12	5.69	0.05	2.41
11	47.4	196	0.491	0.447	1.62	0.19	5.89	0.08	2.49
12	43.4	146	0.444	0.390	1.42	0.14	6.03	0.06	2.55
13	39.4	107	0.401	0.337	1.27	0.11	6.13	0.05	2.60
14	35.4	78	0.361	0.288	1.15	0.08	6.22	0.04	2.63
15	31.4	56	0.325	0.243	1.05	0.07	6.28	0.03	2.66
16	25.4	33	0.275	0.184	0.95	0.08	6.36	0.03	2.69
17	19.4	19	0.231	0.134	0.87	0.06	6.42	0.02	2.72

The batch SC experiments were performed based on the corresponding T and P in each stage for each $(X_B)_0$ in Tables 3-6. The SC experiments for each $(X_B)_0$ were started from the corresponding initial three-phase transformation condition (T_0, P_0) and stopped at the corresponding final three-phase transformation condition (T_N, P_N) when vaporization was no longer observed.

Fig. 6 shows the calculated results of L_n, $S_{tot,n}$, and $V_{tot,n}$ in each stage during the cooling process for L_0=10 g with $(X_B)_0$=0.80, where temperature decreases from T_0=68.6 °C to T_f=16.6 °C. Note that L_n decreases rapidly during the early cooling process and then decreases slowly during the later cooling process; subsequently, $S_{tot,n}$ increases rapidly during the early cooling process and then increases slowly during the later cooling process. Similar results are obtained for L_0=10 g with $(X_B)_0$=0.85-0.95 in Figs. 7-9. And L_n for $(X_B)_0$=0.95 decreases more rapidly during the early cooling process than that for $(X_B)_0$=0.80 and, subsequently, $S_{tot,n}$ for $(X_B)_0$=0.95 increases more rapidly during the early cooling process than that for $(X_B)_0$=080.

According to the calculated results in Tables 3-6, some liquid remains with the final durene crystalline product at the end of SC.

Table 5. Calculated results for L_0=10 g with $(X_B)_0$=0.90 using ΔT=2 °C for n=1-10, ΔT=4 °C for n=11-15, and ΔT=6 °C for n=16-17, respectively

n	T_n (°C)	P_n (Pa)	$(X_B)_n$	$(Y_B)_n$	L_n (g)	S_n (g)	$S_{tot,n}$ (g)	V_n (g)	$V_{tot,n}$ (g)
0	74.1	1,154	0.900	0.902	10.0	0	0	0	0
1	72.1	1,023	0.863	0.864	6.16	2.70	2.70	1.15	1.14
2	70.1	905	0.827	0.827	4.34	1.28	3.98	0.54	1.69
3	68.1	799	0.792	0.790	3.30	0.73	4.71	0.31	2.00
4	66.1	705	0.758	0.754	2.64	0.46	5.17	0.20	2.19
5	64.1	620	0.725	0.719	2.18	0.32	5.49	0.14	2.33
6	62.1	544	0.694	0.684	1.86	0.23	5.72	0.10	2.43
7	60.1	477	0.663	0.649	1.61	0.17	5.89	0.07	2.50
8	58.1	417	0.633	0.616	1.42	0.13	6.02	0.06	2.55
9	56.1	364	0.605	0.583	1.27	0.11	6.13	0.05	2.60
10	54.1	317	0.577	0.550	1.15	0.09	6.21	0.04	2.64
11	50.1	239	0.524	0.488	0.96	0.13	6.35	0.06	2.69
12	46.1	178	0.476	0.428	0.83	0.09	6.44	0.04	2.73
13	42.1	132	0.430	0.373	0.73	0.07	6.51	0.03	2.76
14	38.1	97	0.388	0.321	0.66	0.05	6.56	0.02	2.78
15	34.1	70	0.349	0.273	0.60	0.04	6.60	0.02	2.80
16	28.1	42	0.296	0.209	0.53	0.05	6.65	0.02	2.82
17	22.1	25	0.250	0.155	0.48	0.03	6.68	0.02	2.83

Table 6. Calculated results for L_0=10 g with $(X_B)_0$=0.95 using ΔT=1 °C for n=1-5, ΔT=2 °C for n=6-10, and ΔT=4 °C for n=11-15, and ΔT=6 °C for n=16-17, respectively

n	T_n (°C)	P_n (Pa)	$(X_B)_n$	$(Y_B)_n$	L_n (g)	S_n (g)	$S_{tot,n}$ (g)	V_n (g)	$V_{tot,n}$ (g)
0	76.7	1,347	0.950	0.951	10.0	0	0	0	0
1	75.7	1,270	0.931	0.932	6.05	2.77	2.77	1.18	1.18
2	74.7	1,197	0.911	0.913	4.20	1.30	4.07	0.55	1.73
3	73.7	1,127	0.892	0.894	3.16	0.73	4.80	0.31	2.04
4	72.7	1,061	0.874	0.875	2.50	0.46	5.26	0.20	2.24
5	71.7	999	0.856	0.857	2.05	0.32	5.58	0.13	2.37
6	69.7	883	0.820	0.820	1.47	0.41	5.99	0.17	2.54
7	67.7	780	0.785	0.783	1.13	0.24	6.23	0.10	2.64
8	65.7	687	0.752	0.747	0.91	0.15	6.38	0.07	2.71
9	63.7	604	0.719	0.712	0.76	0.11	6.49	0.05	2.75
10	61.7	530	0.688	0.677	0.65	0.08	6.56	0.03	2.79
11	57.7	406	0.628	0.609	0.50	0.11	6.67	0.05	2.83
12	53.7	308	0.572	0.544	0.40	0.07	6.74	0.03	2.86
13	49.7	232	0.519	0.482	0.34	0.05	6.78	0.02	2.88
14	45.7	173	0.471	0.423	0.29	0.03	6.82	0.01	2.89
15	41.7	128	0.426	0.367	0.26	0.02	6.84	0.01	2.90
16	35.7	80	0.364	0.292	0.22	0.03	6.87	0.01	2.91
17	29.7	49	0.310	0.225	0.19	0.02	6.88	0.01	2.92

Thus, the final product consists of the final durene crystalline product and remaining liquid. The calculated yield for the final product is defined as

$$W_{f,the}=S_{tot,N}+L_N \tag{9}$$

The calculated purity of durene for the final product is given by

$$Z_{B,the}=\frac{S_{tot,N}+L_N(X_B)_N}{S_{tot,N}+L_N} \tag{10}$$

where $S_{tot,N}$ is assumed to consist of durene only and $(X_B)_N$ represents the concentration of durene in the remaining liquid (L_N) at the end of SC.

Fig. 10 shows a comparison among L_N, $S_{tot,N}$, $W_{f,the}$ and $W_{f,exp}$ of the final product for each $(X_B)_0$. Fig. 11 shows a comparison between $Z_{B,exp}$ and $Z_{B,the}$ of the final product for each $(X_B)_0$, where $Z_{B,the}$(T) is plotted against the operating temperature for each $(X_B)_0$. The starting point of $Z_{B,the}$(T) represents the feed purity and initial operating temperature; the ending point refers to the calculated

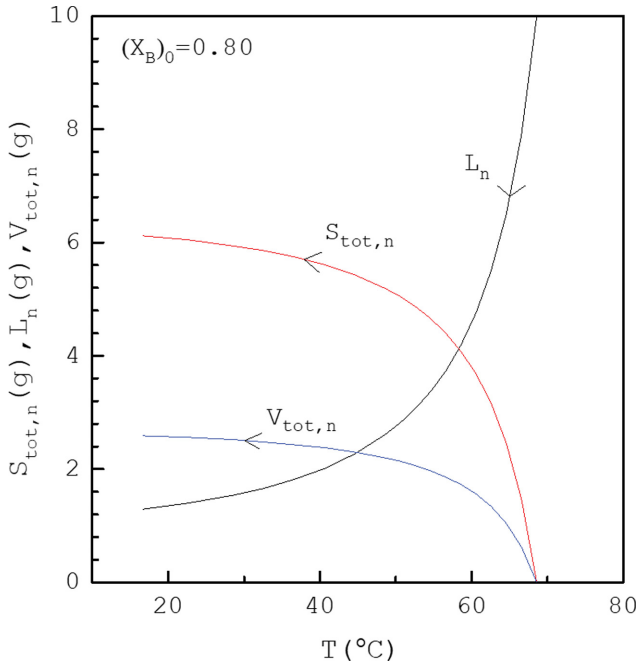

Fig. 6. Calculated results of L_n, $S_{tot,n}$ and $V_{tot,n}$ in each stage during the cooling process for L_0=10 g with $(X_B)_0$=0.80.

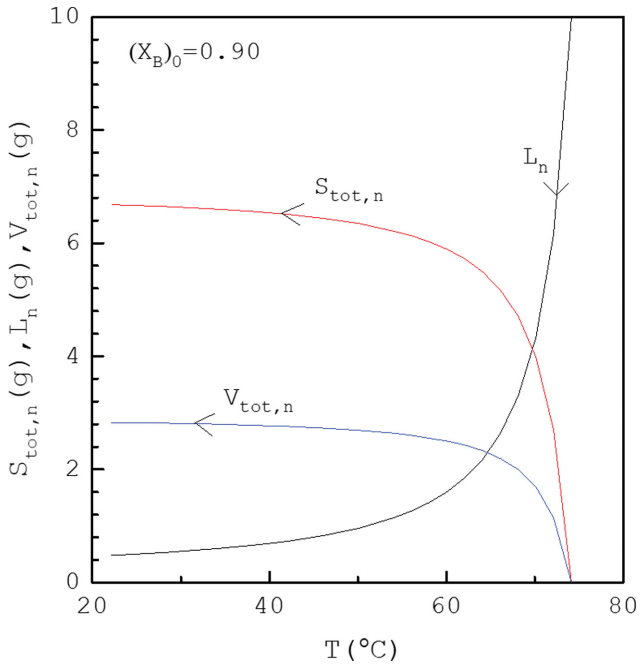

Fig. 8. Calculated results of L_n, $S_{tot,n}$ and $V_{tot,n}$ in each stage during the cooling process for L_0=10 g with $(X_B)_0$=0.90.

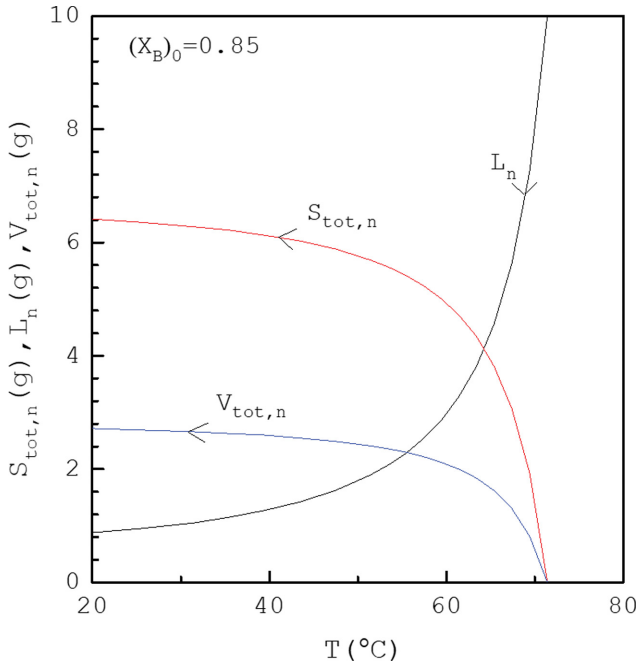

Fig. 7. Calculated results of L_n, $S_{tot,n}$ and $V_{tot,n}$ in each stage during the cooling process for L_0=10 g with $(X_B)_0$=0.85.

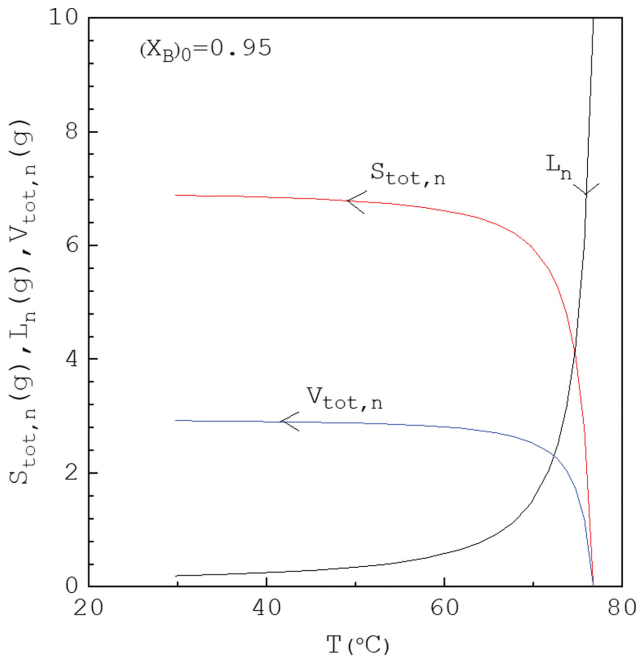

Fig. 9. Calculated results of L_n, $S_{tot,n}$ and $V_{tot,n}$ in each stage during the cooling process for L_0=10 g with $(X_B)_0$=0.95.

product purity and final operating temperature. In Fig. 11, four repetitive experiments were performed to obtain the average values of $W_{f,exp}$ and $Z_{B,exp}$, respectively, for each $(X_B)_0$. In Fig. 10, as $(X_B)_0$ increases from 0.80 to 0.95, L_N decreases from 1.29 g to 0.18 g, while $S_{tot,N}$ increases from 6.12 g to 6.89 g. However, $W_{f,the}$ remains nearly the same regardless of $(X_B)_0$. Thus, for a higher $(X_B)_0$, L_N decreases while $S_{tot,N}$ increases at the end of SC and, consequently, as shown in Fig. 11, a higher $(X_B)_0$ leads to a higher $Z_{B,the}$ due to a smaller L_N in the final product.

By combining Figs. 10 and 11, as SC was operated from 68.6 °C to 16.6 °C, $(X_B)_0$=0.80 was experimentally purified to $Z_{B,exp}$=0.872 with $W_{f,exp}$=5.87 g, as opposed to $Z_{B,the}$=0.863 with $W_{f,the}$=7.41 g. As SC was operated from 71.4 °C to 19.4 °C, $(X_B)_0$=0.85 was experimentally purified to $Z_{B,exp}$=0.914 with $W_{f,exp}$=5.49 g, as opposed to

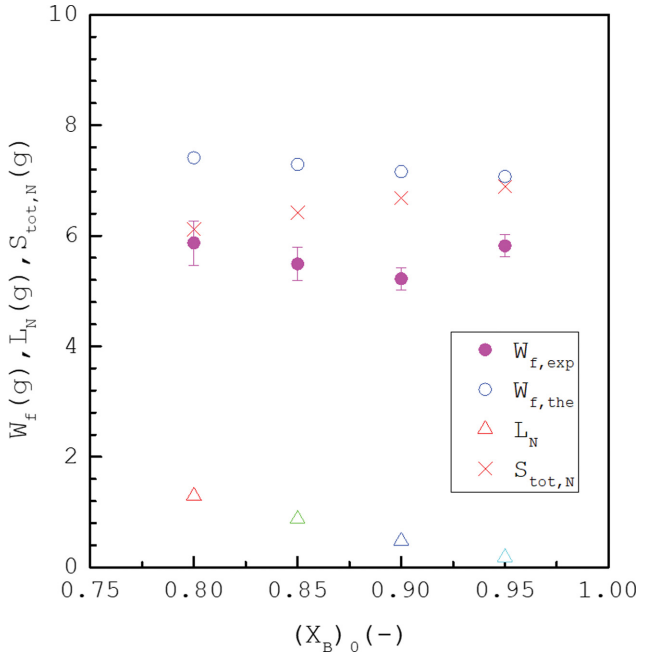

Fig. 10. Comparison among L_N, $S_{tot,N}$, $W_{f,the}$ and $W_{f,exp}$ of the final product for each $(X_B)_0$, where four repetitive experiments were performed to obtain the average value of $W_{f,exp}$ for each $(X_B)_0$ and the error bars represent the 95% confidence interval for $W_{f,exp}$.

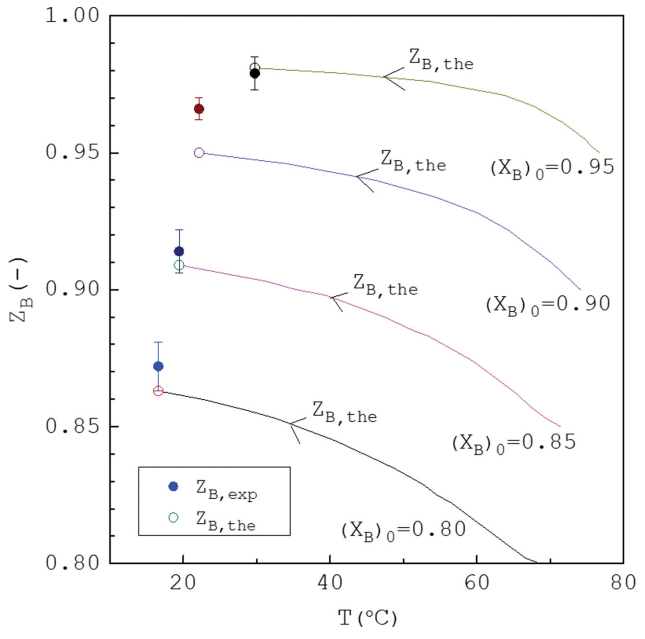

Fig. 11. Comparison between $Z_{B,exp}$ and $Z_{B,the}$ of the final product for each $(X_B)_0$, where four repetitive experiments were performed to obtain the average value of $Z_{B,exp}$ for each $(X_B)_0$ and the error bars represent the 95% confidence interval for $Z_{B,exp}$.

$Z_{B,the}$=0.909 with $W_{f,the}$=7.29 g. As SC was operated from 74.1 °C to 22.1 °C, $(X_B)_0$=0.90 was experimentally purified to $Z_{B,exp}$=0.966 with $W_{f,exp}$=5.22 g, as opposed to $Z_{B,the}$=0.950 with $W_{f,the}$=7.16 g. As SC was experimentally operated from 76.7 °C to 29.7 °C, $(X_B)_0$=0.95 was purified to $Z_{B,exp}$=0.979 with $W_{f,exp}$=5.82 g, as opposed to $Z_{B,the}$=0.981 with $W_{f,the}$=7.07 g. Thus, $Z_{B,exp}$ was slightly greater than $Z_{B,the}$ for $(X_B)_0$=0.80-0.90 while $Z_{B,exp}$ was nearly the same as $Z_{B,the}$ for $(X_B)_0$=0.95; however, $W_{f,exp}$ was generally lower than $W_{f,the}$ for each $(X_B)_0$.

Discrepancies between the calculated and experimental results of product yield and purity are attributed to (a) the calculated results being obtained based on the assumption that each stage was operated at the three-phase transformation; however, this might not always be achieved during the experiments; (b) liquid inclusion might occur in the formation of the durene crystalline product; and (c) isodurene might be incorporated into the durene crystalline product due to the similar molecular structure between durene and isodurene.

CONCLUSIONS

SC was successfully applied to purify durene from a mixture consisting of isodurene and durene. A model based on the mass and energy balances was proposed to determine the variation of the amount of the durene crystalline product, remaining liquid and produced vapor via a series of three-phase transformations during SC. The results indicated that the experimental purity of the final product was close to that predicted by the model, while the experimental yield of the final product was lower than that predicted by the model. Compared to conventional melt crystallization, neither solid/liquid separation nor crystal washing is required for SC when all the liquid is vaporized and no mother liquor adheres to the final solid product at the end of SC.

ACKNOWLEDGEMENTS

The author would like to thank Ministry of Science and Technology of Taiwan (MOST108-2221-E-182-034-MY2) and Chang Gung Memorial Hospital (CMRPD2K0011) for financial support of this research. The author also expresses his gratitude to Wei-Chen Fan and Keng-Fu Liu for their experimental work.

NOTATION

L_0 : mass of the initial liquid feed [g]
L_n : mass of the liquid out of stage n [g]
P_n : pressure in stage n [Pa]
P_j^{sat} : saturated vapor pressure of component-j [Pa]
$P_{tri,j}$: triple-point pressure of component-j [K]
R : ideal gas constant [8.314 J/mol-K]
S_n : mass of the durene crystalline product formed in stage n [g]
$S_{tot,n}$: total amount of the durene crystalline product formed from stage 1 to stage n [g]
T_{eu} : eutectic temperature [K]
T_n : temperature in stage n [K]
$T_{b,j}$: boiling temperature of component-j [K]
$T_{m,j}$: melting temperature of component-j [K]
$T_{tri,j}$: triple-point temperature of component-j [K]
t : time [sec]

V_n : mass of the vapor formed in stage n [g]
$V_{tot,n}$: total amount of vapor formed and removed from stage 1 to stage n [g]
$W_{f,exp}$: measured weight of the final product at the end of SC [g]
$W_{f,the}$: calculated weight of the final product at the end of SC [g]
$(X_j)_0$: initial mole fraction of component-j in the liquid feed, dimensionless
$(X_j)_n$: mole fraction of component-j in the remaining liquid in stage n, dimensionless
$(Y_j)_n$: mole fraction of component-j in the vapor phase out of stage n, dimensionless
$Z_{B,exp}$: experimental purity of durene in the final product, dimensionless
$Z_{B,the}$: calculated purity of durene in the final product, dimensionless
$\Delta H_{m,j}$: heat of melting for component-j (>0) [J/mol]
$\Delta H_{V,j}$: heat of vaporization for component-j (>0) [J/mol]

Subscript

0 : in the initial feed
f : at the end of SC
n : in stage
N : in the last stage

REFERENCES

1. R. E. Kirk and D. F. Othmer, *Encyclopedia of chemical technology*, Vol. 4, John Wiley & Sons Inc., New York (1991).
2. S. Cong, Y. Liu, H. Li, X. Li, L. Zhang and L. Wang, *Chin. J. Chem. Eng.*, **23**, 505 (2015).
3. L. D. Shiau, C. C. Wen and B. S. Lin, *Ind. Eng. Chem. Res.*, **44**, 2258 (2005).
4. L. D. Shiau, C. C. Wen and B. S. Lin, *AIChE J.*, **52**, 1962 (2006).
5. L. D. Shiau, C. C. Wen and B. S. Lin, *AIChE J.*, **54**, 337 (2008).
6. L. D. Shiau and K. F. Liu, *Ind. Eng. Chem. Res.*, **52**, 1716 (2013).
7. L. D. Shiau, *Sep. Purif. Technol.*, **255**, 117688 (2021).
8. L. D. Shiau and C. C. Yu, *Sep. Purif. Technol.*, **66**, 422 (2009).
9. L. D. Shiau, K. F. Liu and Y. C. Hsu, *Chem. Eng. Res. Des.*, **117**, 301 (2017).
10. L. D. Shiau, *Cryst. Growth Des.*, **20**, 1328 (2020).
11. K. J. Kim and J. Ulrich, *J. Colloid Interface Sci.*, **252**, 161 (2002).
12. J. Ulrich and H. Glade, *Melt crystallization: fundamentals, equipment and applications*, Shaker Verlag, Germany (2003).
13. Q. Li, Z. Yi, X. Sun and M. Su, *Korean J. Chem. Eng.*, **27**(2), 619 (2010).
14. X. Jiang, B. Hou, G. He and J. Wang, *Chem. Eng. Sci.*, **84**, 120 (2012).
15. T. Beierling, J. Osiander and G. Sadowski, *Sep. Purif. Technol.*, **118**, 13 (2013).
16. J. Micovic, T. Beierling, P. Lutze, G. Sadowski and A. Gorak, *Chem. Eng. Process: Process Intensif.*, **67**, 16 (2013).
17. X. Jiang, M. Li, G. He and J. Wang, *Ind. Eng. Chem. Res.*, **53**, 13211 (2014).
18. K. Fukui, T. Fujikawa, H. Satone, T. Yamamoto and K. Maeda, *Chem. Eng. Sci.*, **143**, 114 (2016).
19. M. Ahmad and J. Ulrich, *Chem. Eng. Technol.*, **39**, 1341 (2016).
20. N. Yazdanpanah, A. Myerson and B. Trout, *Ind. Eng. Chem. Res.*, **55**, 5019 (2016).
21. I. S. Ioannou, S. S. Kontos, P. G. Koutsoukos and C. A. Paraskeva, *Sep. Purif. Technol.*, **197**, 8 (2018).
22. S. Jia, B. Jing, Z. Gao, J. Gong, J. Wang and S. Rohani, *Sep. Purif. Technol.*, **259**, 118140 (2021).
23. P. J. Linstrom and W. G. Mallard, Ed. NIST Chemistry WebBook, NIST Standard Reference Database Number 69, National Institute of Standards and Technology, MD, USA (2018).
24. J. M. Smith, H. C. Van Ness and M. M. Abbott, *Introduction to chemical engineering thermodynamics*, McGraw-Hill Book Co., Singapore (2001).
25. S. I. Sandler, *Chemical, Biochemical, and Engineering Thermodynamics*, John Wiley & Sons Inc., Asia (2006).